HHS Public Access

Author manuscript

Cancer Gene Ther. Author manuscript; available in PMC 2010 June 01.

Published in final edited form as:

Cancer Gene Ther. 2009 December ; 16(12): 923–935. doi:10.1038/cgt.2009.34.

Anti-cancer oncolytic activity of respiratory syncytial virus

I Echchgadda[2,#], **S Kota**[1,#], **I DeLa Cruz**[2], **A Sabbah**[1], **T Chang**[1], **R Harnack**[1], **V Mgbemena**[1], **B Chatterjee**[2,3,*], and **S Bose**[1,*]

[1] Department of Microbiology and Immunology, The University of Texas Health Science Center at San Antonio, San Antonio, Texas

[2] Department of Molecular Medicine/Institute of Biotechnology, The University of Texas Health Science Center at San Antonio, San Antonio, Texas

[3] South Texas Veterans Health Care System, San Antonio, Texas

Abstract

Oncolytic virotherapy is an emerging bio-therapeutic platform for cancer treatment, which is based on selective infection/killing of cancer cells by viruses. Herein we identify the human respiratory syncytial virus (RSV) as an oncolytic virus. Using prostate cancer models, we show dramatic enhancement of RSV infectivity *in vitro* in the androgen-independent, highly metastatic PC-3 human prostate cancer cells compared to the non-tumorigenic RWPE-1 human prostate cells. The oncolytic efficiency of RSV was established *in vivo* using human prostate tumor xenografts in nude mice. Intra-tumoral and intra-peritoneal injections of RSV led to a significant regression of prostate tumors. Furthermore, enhanced viral burden in PC-3 cells led to selective destruction of PC-3 cancer cells *in vitro* and in xenograft tumors *in vivo* due to apoptosis triggered by the down-regulation of NF-κB activity (and the resulting loss of anti-apoptotic function of NF-κB) in RSV-infected PC-3 cells. The intrinsic (mitochondrial) pathway constitutes the major apoptotic pathway; however, the death-receptor-dependent extrinsic pathway, mediated by the paracrine/autocrine action of tumor necrosis factor-α produced from infected cells, also partly contributed to apoptosis. Thus, the oncolytic property of RSV can potentially be exploited to develop targeted therapeutics for the clinical management of prostate tumors.

Keywords

Oncolytic; respiratory syncytial virus; anti-cancer; prostate cancer; apoptosis

Correspondence (for correspondence with the editor and for proofs): Santanu Bose, Ph.D., Department of Microbiology & Immunology, The University of Texas Health Science Center at San Antonio, 7703 Floyd Curl Drive, MC-7758, San Antonio, TX 78229. Telephone: (210) 567 1019, E-mail: bose@uthscsa.edu, Bandana Chatterjee, Ph.D., Department of Molecular Medicine/ Institute of Biotechnology, The University of Texas Health Science Center at San Antonio, 15355 Lambda Drive, San Antonio, TX 78245. E-mail: chatterjee@uthscsa.edu.

[#]These authors contributed equally to this work

Introduction

Oncolytic virotherapy, based on selective infection and “killing” of cancer cells by viruses, is an emerging bio-therapeutic platform for cancer treatment (1–4). Due to enhanced viral burden in tumor cells (not in normal cells), cancer cells are ablated by necrosis or apoptosis. Oncolytic viruses identified to date are: adenovirus, reovirus, herpes simplex virus (HSV), Newcastle disease virus (NDV), vaccinia virus, myxoma virus, influenza virus, measles virus, coxsackievirus and vesicular stomatitis virus (VSV). Recent studies have revealed that one virus type may not be sufficient to treat cancer efficiently. A repertoire of numerous oncolytic viruses (with different modes of action) may be required to treat aggressive cancers. Combined use of different classes of oncolytic viruses for cancer therapy appears to be much more efficacious than use of a single virus class. Human respiratory syncytial virus (RSV) is a respiratory tract-specific enveloped virus and as a non-segmented negative sense single stranded RNA (NNS) virus, it belongs to the paramyxovirus family (5,6). RSV infects cells via direct fusion of viral envelope with the plasma membrane. Viral RNA genome undergoes transcription/replication in the cytoplasm without nuclear involvement. The paramyxovirus measles and NDV possess oncolytic activity (7–9). Whether RSV is an oncolytic virus, however, has not been addressed.

Resistance to apoptosis or “programmed cell death” (10, 11) is the hallmark of most advanced-stage tumors, which do not respond to radio- and chemotherapy. Two major pathways, intrinsic and extrinsic, are involved in the induction of apoptosis (10, 11). Both pathways are regulated by caspases, which are a family of cysteine proteases that exist as inactive pro-enzymes (12). The extrinsic pathway is mediated following caspase-8 activation, which is initiated in response to the binding of death receptors [tumor necrosis factor (TNF) receptor, Fas, TRAIL-receptor 1 &2] to cognate ligands [TNF, Fas ligand (FasL), TRAIL]. Various signals/stimuli trigger the intrinsic pathway. Activation of this pathway results in release of apoptotic factors such as cytochrome c from the mitochondria and subsequent activation of caspase-9 (13). Both intrinsic and extrinsic pathways converge to activate executioner caspases (caspase-3, -6, and -7), which are responsible for the characteristic morphological changes of apoptosis (14). NF-κB- and Akt-mediated signaling plays an important role in cell survival by inducing anti-apoptotic genes and repressing pro-apoptotic genes. Induction of NF-κB DNA-binding activity and phosphorylation of Akt [through activation of the upstream phosphoinositide-3 (PI3) kinase (PI3-kinase)] result in the activation/expression of anti-apoptotic molecules. Inhibition of NF-κB/Akt activation normally commits cells to apoptosis (15, 16). Due to the anti-apoptotic activity of cancer cells, it is a good target for oncolytic viruses. For example, cancer cells that lack p53 expression are highly susceptible to E1B protein deleted adenoviruses (17, 18). In addition, since anti-viral response against RNA viruses (like paramyxoviruses) is coupled with the pro-apoptotic pathway, viruses can multiply robustly in cancer cells due to lack of pro-apoptotic (and anti-viral) signaling. Increased viral burden results in apoptosis of cancer cells.

Metastatic prostate cancer is a leading cause of cancer deaths in men in the United States. Prostate cancer cells are initially androgen-dependent for growth and proliferation, so that androgen ablation therapy can be successfully implemented to destroy prostate cancer cells

by apoptosis. Relapsed tumors, however, are therapy resistant due to androgen independence and apoptosis resistance (19). We utilized prostate cancer model to investigate the ability of RSV to cause oncolysis because majority of prostate tumors harbor defective NF-κB pathway (20, 21). Since NF-κB also plays a critical role during anti-viral response against RSV, we argued that deregulated NF-κB activation status may result in functioning of RSV as an oncolytic virus against prostate tumors.

Herein we show that RSV is an oncolytic virus and demonstrate its oncolytic activity against androgen-independent prostate tumors derived from PC-3 human prostate cancer cells. PC-3 cells are poorly differentiated and highly tumorigenic, showing aggressive migratory (metastasis) behavior in culture (22) and in tumor xenografts grown in nude mice (23). Our results reveal that RSV infectivity is markedly enhanced in PC-3 cells compared to that in the non-tumorigenic RWPE-1 (RWPE) human prostate epithelial cells. Enhanced viral burden in PC-3 cells resulted in selective apoptosis-induced loss of the cancer cells *in vitro* and *in vivo*, causing regression of PC-3 cell-derived xenograft tumors in immune-deficient nude mice. We show that RSV induces apoptotic activity in PC-3 cells by activating caspase-3 through the intrinsic pathway. Additionally, the extrinsic pathway, induced by the autocrine/paracrine action of tumor necrosis factor-α (TNF) produced from RSV-infected cells, plays a partial role in the virus-induced apoptosis. We further show that the RSV-mediated loss of the anti-apoptotic function of NF-κB in PC-3 cells was associated with apoptosis in a caspase-3- dependent manner.

Materials and Methods

Virus, cells, pharmacologic inhibitors

RSV (A2 strain) was propagated in CV-1 cells. Viral titer was monitored by plaque assay (24–26). RWPE, PC-3 and LNCAP cells were from ATCC. Apoptosis inhibitors for caspase -3 (Z-DQMD-FMK), -8 (Z-IETD-FMK), -9 (Z-LEHD-FMK), -3/7 (Z-DEVD-FMK), and the control inhibitor (Z-FA-FMK) were from Calbiochem. Caspase-12 inhibitor (Z-ATAD-FMK) was purchased from MBL. The Akt inhibitor wortmannin was from Calbiochem and a second Akt inhibitor (1L6-Hydroxymethyl-chiro-inositol-2-(R)-2-O-methyl-3-O-octadecylcarbonate) was from MBL International.

RSV infection

RSV (0.2 or 2 MOI) was added to cells for adsorption at 37°C for 1.5h and following washing, infection was continued for additional 4h–42h. At various times post-infection, culture supernatants were assayed for virus yield by plaque assay. Cell morphology was visualized microscopically.

Apoptosis and cell viability

Cells infected with RSV for 36h, were examined for apoptosis and cell viability. Cell cytotoxicity of infected cells was quantified by enumerating viable cells using MTT assay (27). To assess apoptosis, dissociated cells were fixed with cold ethanol and analyzed by TUNEL assay (Roche, Germany). DNA in apoptotic nuclei, with incorporated fluorescein-labeled nucleotides, was analyzed by FACS. Apoptosis analysis was also performed using

the annexin V/propidium iodide apoptosis detection kit (BioVision). Apoptosis in tumors was visualized by examining annexin V labeling of single cell suspensions prepared from surgically excised tumors (28). Dunnett's two-sided 99% and 95% Simultaneous Confidence Interval (SCI) Test was used to compare statistical significant difference between the mean of reference treatment group and the mean of the other treatment groups.

Assay for roles of various caspases; roles for Akt and NF-κB signaling

PC-3 cells were pre-treated with specific caspase inhibitor(s) for 1h at 37°C. Caspase-3, -8, -9 and -3/7 inhibitors at 15 μM–60 μM were used. The caspase-12 inhibitor was used at 50 μM–100 μM. RSV was added to cells for adsorption at 37°C for 1.5h. Infection in the washed cells continued for additional 36h in the presence of inhibitors, and then cells were analyzed for apoptosis.

For neutralization (29), PC-3 cells were infected with RSV in the presence of 900 ng/ml of interleukin-1β (IL-1) or TNF-neutralizing antibodies (R&D systems). At 36h post-infection, cells were assayed for apoptosis. PC-3 and RWPE cells were pre-treated with either SN50 peptide (30 μM) or control SN50M (50 μM) peptide (Calbiochem) for 2h, followed by virus infection (in the presence of peptides) for 0–36h, after which apoptosis was measured.

Involvement of Akt in apoptosis was examined using wortmannin (Calbiochem) and a second Akt inhibitor from MBL International. Cells pre-treated with either wortmannin (200 nM) or Akt inhibitor (20 μM) were infected with RSV (in the continued presence of the inhibitor) for 0 – 36h, followed by analysis for apoptosis.

Reverse transcription-PCR (RT-PCR)

Total cellular RNAs isolated from RSV-infected PC-3 cells/tumors were reverse transcribed and cDNAs were analyzed for human and mouse TNF and GAPDH by PCR. RSV nucleocapsid protein (N protein) primer was also utilized to detect N expression in tumors and various mice organs. The primers used to detect the indicated genes by RT-PCR are shown below.

GAPDH forward, 5′-GTCAGTGGTGGACCTGACCT, *GAPDH reverse*, 5′-AGGGGTCTACATGGCAACTG; *RSV-N forward*, 5′-AAGGGATTTTTGCAGGATTGTTT, *RSV-N reverse*, 5′-TCCCCACCGTAACATCACTTG; human *TNF-α forward*, GAGTGACAAGCCTGTAGCCCATGTTGTAGCA, human *TNF-α reverse*, *GCAATGATCCCAAAGTAGACCTGCCCAGACT; mouse TNF-α forward*, *CCTGTAGCCCACGTCGTAGC*, *mouse TNF-α reverse*, TTGACCTCAGCGCTGAGTTG.

Western blot and EMSA

Mock-infected or RSV- infected PC-3 cell lysates (50 μg) or tumor homogenates (100 μg) were analyzed by SDS-PAGE (7.5% or 15%) and Western blotting. Sources of antibodies: Bcl-2, Bcl-xL, Bad, Bax; phospho-Akt, Akt from Cell Signaling Technology. Caspase-3, PARP-1, GFP and Heat shock protein-70, β-actin from Santa Cruz Biotechnology. For EMSA, nuclear extracts from infected cells were incubated with ^{32}P-labeled NF-κB

oligonucleotide (from the IL6 promoter) and protein-DNA complex was analyzed as before (24).

Prostate cancer xenograft tumors in nude mice

7-week-old athymic nude mice (Jackson Laboratory) were subcutaneously injected with PC-3 cells (2×10^6 cells in 100μl) at a site below the ear (30). When tumor size reached 150–200 mm^3, RSV (1×10^6 pfu per animal) or Opti-MEM (carrier control) was injected I.T or I.P. At 2-day intervals, RSV was injected for 8–14 days. Tumor volumes were measured till 35–38d post-infection. Tumor bearing mice were also injected (I.T or I.P) with GFP-RSV. At 16h post-infection, following euthanization, tumors were surgically excised and tumor homogenate was prepared with Trizol or PBS for RNA and protein extraction, respectively.

Results

RSV-induced oncolysis of human prostate cancer cells

Selective enhancement of RSV infectivity (at 36h post-infection) in PC-3 cells over RWPE-1 (RWPE) non-malignant prostate cells is shown in Figure 1. RSV infection was dramatically augmented (approximately 2000–2500 folds) in PC-3 cancer cells compared to non-tumorigenic RWPE cells (Figure 1a). High viral burden led to extensive loss of viable PC-3 cells, whereas RWPE cells showed only limited loss of viability, revealed by MTT assay (Figure 1b). The much greater cytopathic effect and loss of cell viability of RSV infected (at 24h post-infection) PC-3 cells compared to RWPE cells is shown by the significantly higher cell death, evident from cell rounding and loss of normal cellular morphology (Figure 1c). The oncolytic effect of RSV is specific, since human parainfluenza virus-3 (a RSV related paramyxovirus) (25, 29) failed to replicate efficiently in PC-3 cells and did not promote loss of cell viability (Supplementary Figure S1). The enhanced viral infectivity and associated robust RSV growth *in vitro* in cancer cells compared to normal cells strongly implicated RSV as an oncolytic virus.

Viability of the androgen-dependent LNCaP human prostate cancer cells was also markedly reduced when infected with RSV within 10h post-RSV infection (Figure 1d). In fact, the oncolytic activity was more significant in LNCaP cells compared to PC-3 cells. The oncolytic activity of RSV was not limited to human cancer cell-lines, since the murine prostate cancer epithelial cells, RM1 cells infected with RSV showed enhanced cellular death similar to infected PC-3 and LNCap cells (Fig. 1e). However, since PC-3 cells are androgen-insensitive cancer cell line bearing a highly aggressive migratory phenotype and are resistant to androgen ablation therapy, we decided to utilize PC-3 cells for further studies aimed at establishing RSV as an oncolytic virus.

The oncolytic effect of RSV on human prostate tumor xenografts

A human prostate tumor xenograft model (30) was used to examine the oncolytic function of RSV *in vivo* (Figure 2). Administration of RSV to the subcutaneously produced PC-3 tumors via intra-tumoral injection (I.T) led to a drastic reduction in tumor mass (Figure 2a). In contrast, the size of the non-infected tumors (carrier control) continued to increase with

time. Representative photographic documentation of tumor regression below the ear resulting from RSV infection (I.T administration) is shown (Figure 2b).

We also investigated the efficacy of intraperitoneally (I.P) delivered RSV for causing tumor regression and determined that intraperitoneally injected RSV also rendered significant reduction in the tumor growth compared to the growth of control, medium-treated tumors (Figure 2c). The significant tumor regression by intraperitoneally delivered RSV is shown in Figure 2d. Similar results were obtained with tumors grown in the dorsal flank (Supplementary Figure S2). Therefore, the RSV-responsive restriction of tumor growth at two sites (ear and flank) demonstrates the versatility of RSV in conferring oncolysis *in vivo* at different anatomical regions.

Notably, a high dose of RSV injection by I.P (10^6 pfu/mouse; eight injections at 2d intervals) in control nude mice (with no tumor burden), did not affect the normal health status of the animals even after 2 months following RSV injection (not shown). This indicates that RSV is ineffective in causing systemic infection and is consistent with its property as a lung-tropic virus, known for specific infectivity to the airway lumen. Taken together, these results suggest that RSV gets concentrated in the tumor micro-environment to infect and destroy cancer cells in a host animal environment, while normal cells of nonmalignant tissues are spared from the viral assault. These results also underscore the potential value of RSV as a systemically deliverable oncolytic virus in prostate cancer treatment.

Targeting of RSV to prostate tumors

To demonstrate tumor-specific targeting/localization of systemically administered RSV, tumor-bearing animals were injected (I.P) with green fluorescent protein (GFP) expressing RSV (GFP-RSV) (31). This recombinant virus harbors the GFP cDNA fused to the viral genome. Therefore, GFP expression can occur only following infection. Mice bearing subcutaneous prostate tumors were injected either with medium (control mock infection) or GFP-RSV via I.T or I.P injections, and tumors were surgically excised from the euthanized mice. Western blot of tumor homogenates with anti-GFP antibody revealed GFP expression in the tumors of infected mice (Figure 3a), demonstrating RSV localization at the tumor site. The tumor specific targeting of RSV was also established by monitoring the presence of RSV in various organs of infected mice. RSV infection of tumor bearing mice by either I.T or I.P route resulted in the specific targeting of the virus to the tumor as revealed by performing viral infection assay with tumor homogenates (Fig. 3b, 3c). In contrast, we failed to detect any virus in various organs (lungs, liver, kidney, spleen) of these animals (Fig. 3b, 3c). The absence of RSV in these organs was further validated by the failure to detect RSV nucleocapsid (N protein) protein mRNA expression in these organs (Fig. 3d). These results demonstrated that I.T and I.P administration of RSV cumulates in specific targeting of RSV to the tumors in the absence of viral dissemination to various organs of the infected animals.

Role of the mitochondria-dependent intrinsic pathway in RSV-induced apoptosis of prostate cancer cells

Loss of viability of RSV-infected PC-3 cells (Figures 1b and 1c) was due to apoptosis, as shown by TUNEL assay, which detects late apoptotic events (Figure 4a, left panel). Apoptosis was markedly higher for RSV-infected PC-3 cells compared to that of the infected RWPE cells. Annexin V staining (signifying early apoptosis) confirmed RSV-induced apoptosis of PC-3 cells (Figure 4a, right panel). Annexin V labeled ~52% of RSV-infected PC-3 cells compared to mere 0.2% labeling of RWPE cells (lower right quadrant), indicating RSV-induced early apoptosis selectively in the cancer cells. The kinetics of apoptosis induction by RSV in PC-3 cells revealed that apoptosis is stimulated at 8h post-infection and the it is sustained even at 36h post-infection (Fig. 4b).

Since caspase-3 plays a central role in apoptosis, we investigated whether the virus infection would result in caspase-3 activation. PC-3 cells infected with RSV for 8h and 16h were analyzed by Western blotting using an anti-caspase-3 antibody that recognizes both the full-length and cleaved caspase-3 protein (Figure 4c). While mature full-length pro-caspase-3 was detected in mock infected cells, RSV infection was associated with loss of pro-caspase-3 (and appearance of cleaved caspase-3 protein), demonstrating the ability of RSV to cleave the zymogen to activate caspase-3 in PC-3 cells.

Caspase-3 activation in the intrinsic apoptotic pathway is regulated by Bcl-2 protein family, which includes a number of pro-apoptotic (e.g. Bax and Bad) and anti-apoptotic (e.g. Bcl-2 and Bcl-xL) proteins which regulate mitochondria-mediated apoptosis. We examined the expression of these proteins in RSV-infected PC-3 cells to study their role in apoptosis. While gradual decreased expression of the anti-apoptotic proteins (Bcl-2 and Bcl-xL) following RSV infection was observed (Figure 4d), the expression of the pro-apoptotic proteins (Bad and Bax) increased steadily in virus-infected cells (Figure 4e). Please note that appearance of pro-apoptotic genes (Bax and Bad genes) (Fig. 4e) and disappearance of anti-apoptotic genes (Bcl-xl and Bcl-2 genes) (Fig. 4d) coincides with the time-frame (around 8h–10h post-infection) of apoptosis induction in RSV infected PC-3 cells (Fig. 4b). Pre-dominance of the pro-apoptotic over anti-apoptotic signals indicates the importance of mitochondria-mediated apoptosis (intrinsic pathway) in the caspase-3 activation in RSV-infected cells.

Role of the death-receptor (extrinsic pathway) and caspase-12-mediated (ER-stress pathway) apoptosis of RSV-infected cancer cells

The extrinsic pathway to apoptosis results from the engagement of death receptors (e.g. TNF-receptor and Fas) with cognate ligands (TNF and FasL) leading to caspase-8 activation (10, 11). The ER-stress pathway (32) activation leads to the activation of caspase-12. Activation of both caspase-8 and caspase-12 results in caspase-3 activation. In order to explore the contribution of the non-intrinsic pathway in apoptosis induction by RSV, we conducted the infection experiments in the presence of various cell-permeable, irreversible caspase inhibitors (please see the methods section for details). PC-3 cells treated with control and caspase-3, -9, -8, and -12 inhibitors were infected with RSV and at 36h post-infection cellular apoptosis was examined. As expected, inhibition of caspase-3 resulted in a

drastic decline (by 85%) in apoptosis (Figure 5a). Similarly, blocking caspase-9 activity also led to significant inhibition (by 75%) in apoptosis (Figure 5a). These results confirm our data (Figure 4) showing activation of the intrinsic pathway (involving activation of caspase-9 and caspase-3) as the major route to RSV-induced apoptosis. In contrast to caspase-3 and -9, inhibition of caspase-12 did not alter apoptosis in virus- infected cells (Figure 5a). The caspase-12 inhibitor was active since it inhibited RSV- mediated apoptosis significantly (by 40%) in A549 human lung carcinoma cells (data not shown). Involvement of caspase-12 in RSV-infected A549 cells was previously demonstrated (33). It was interesting to note that inhibition of caspase-8 was associated with 15% reduction in apoptosis (Figure 5a). This result suggested that the extrinsic pathway may play a minor role in RSV-mediated apoptosis. The activity of the caspase-8 inhibitor is evident from its efficacy in reducing interferon-γ + Fas antibody mediated apoptosis (34) in A549 cells by 60% (data not shown). During the caspase inhibitor studies, 15 μM inhibitor concentration was optimal for inhibiting apoptosis mediated by caspase-3, -9 and -8, since higher concentration (20 μM – 60 μM) did not augment apoptotic inhibitory activity (data not shown). Similarly, a high concentration (up to 100 μM) of caspase-12 failed to inhibit apoptosis in infected PC-3 cells (data not shown). Treatment of the cells with the caspase inhibitors did not affect cell viability within the experimental time frame in our study (data not shown).

Previous studies had shown that RSV infection of A549 lung carcinoma cells results in the production of TNF and TNF can cause apoptosis in these cells (35). Therefore, we speculated that caspase-8 dependent apoptosis may be mediated by the autocrine/paracrine action of TNF produced from infected PC-3 cells. Indeed, infection of PC-3 cells led to TNF mRNA (Figure 5b) and protein (Supplementary Figure S3) expression as early as 8h post-infection. Secreted TNF plays an important role in activation of extrinsic pathway, since incubation of infected PC-3 cells with TNF neutralizing antibody revealed decreased apoptosis by 15% (Figure 5c). This reduction was similar to the extent of the decline in apoptosis that was observed in response to the caspase-8 inhibition. No further inhibition of apoptosis in cells treated with both TNF neutralizing antibody and caspase-8 inhibitor was observed. This result demonstrates that the minor extrinsic pathway involving activated caspase-8 is exclusively induced via the paracrine/autocrine action of TNF generated by the infected cells. Therefore, TRAIL and/or FasL may not be involved in the induction of the extrinsic apoptotic pathway. Our results show a minor role of the extrinsic pathway in apoptosis, since apoptosis declined dramatically in cells incubated with both the TNF neutralizing antibody and caspase-3 inhibitor (Figure 5c). This decline was due to the inability of activated caspase-9 (induced through the intrinsic pathway) to activate caspase-3 and subsequent apoptosis.

RSV-induced apoptosis in vivo in prostate tumors

To examine the patho-physiological relevance of apoptosis induced by the oncolytic activity of RSV, we studied apoptosis in tumors isolated from mice injected with RSV. Mice bearing prostate tumors near the ear were injected with RSV via I.T or I.P (as described above) and at 16h post-infection, tumors were surgically removed from the euthanized mice. Cell suspensions from the tumors were analyzed for apoptosis. Annexin V staining revealed 5%–

7.5% apoptotic cells in control tumors (mice injected with control medium); in contrast, 35%–42% and 22%–26% of tumor cells were apoptotic following I.T or I.P injection of RSV, respectively (Figure 6a). We also show that both intrinsic and extrinsic pathways are operative during apoptosis of the infected tumors. Activation of the intrinsic pathway is evident from expression of the pro-apoptotic Bax protein in the virus-infected (infected via I.T) tumors (Figure 6b). In contrast, anti-apoptotic Bcl-xL protein expression was suppressed following I.T infection (Figure 6c). Similarly, the extrinsic pathway may be induced, since we detected TNF expression in the RSV-infected tumors (via I.T) (Figure 6d) which, based on our *in vitro* results (Figure 5), will act in a paracrine/autocrine mode to activate the extrinsic pathway. Similar results were observed when RSV was injected to the tumor-bearing mice via the I.P route (data not shown). Thus, RSV-infected tumors undergo apoptosis, which then leads to the tumor mass regression.

Role of NF-κB and Akt in the apoptosis of RSV-infected prostate cells

Previous studies with lung cancer cells and with granulocytes showed that RSV-induced apoptosis is associated with changes in Akt and NF-κB activity (36, 37). Therefore, we investigated whether these molecules contribute to the RSV-mediated apoptosis of prostate cancer cells. EMSA revealed activation (as early as 1h post-infection) of NF-κB in RSV-infected RWPE cells (Figure 7a, top panel). In contrast, only marginal activation of NF-κB over the basal NF-κB activity was observed in the RSV-infected PC-3 cells at 1 h (Figure 7a, bottom panel). High basal NF-κB activity in PC-3 cells was previously reported (38). By 6h post-infection, NF-κB activity in PC-3 cells diminished markedly, whereas RSV-infected RWPE cells displayed sustained NF-κB activity at 6h and 10h post-infection (Figure 7a). It is important note that drastic loss of NF-κB activity in infected (at 6h–10h post-infection) PC-3 cells (Fig. 7a) is not due to unequal nuclear extract loading during EMSA, since we demonstrate that equal amounts of nuclear marker protein HDAC-2 is present in all samples corresponding to the samples used for the EMSA assay (Supplementary Figure S4a). The NF-κB-specific cell-permeable inhibitory peptide SN50 (blocks nuclear translocation of NF-κB) (39, 40) induced apoptosis of the infected RWPE cells (Figure 7b). Similarly, SN50 treatment caused significantly enhanced apoptosis of PC-3 cells during early infection time periods (12h post-infection) (Figure 7c). The SN50 effect was specific, since the control SN50M peptide had no effect on apoptosis. We also show that SN50 (but not control peptide) treatment diminishes activated NF-κB in PC-3 cells following 12h post-infection (Supplementary Figure S4a). In addition, SN50 inhibited NF-κB activation in RWPE and PC-3 cells (Supplementary Figure S4b, S4c). A second NF-κB inhibitor PDTC showed similar results (data not shown). The ability of RSV to diminish NF-κB activity in PC-3 cells is independent of apoptosis, since treatment of cells with general pan-caspase inhibitor zVAD did not rescue NF-κB activity in infected cells (Supplementary Figure S5). These results indicate that the anti-apoptotic function of NF-κB determines the apoptotic fate of the infected prostate cells. We conclude that the infected RWPE cells did not undergo apoptosis due to the failure of RSV to block NF-κB activity, while the ability of RSV to down-regulate NF-κB activity in PC-3 cells led to the apoptosis and oncolysis of these cells following infection. The differential modulation of NF-κB activity could be directly attributed to difference in RSV load in PC-3 vs. RWPE cells.

In contrast to NF-κB, RSV marginally activated Akt (based on the phosphorylated Akt to total Akt protein ratio) in RWPE (data not shown) and PC-3 (Supplementary Figure S6) cells. Furthermore, two Akt inhibitors, wortmannin (from Calbiochem) and Akt inhibitor (from MBL), did not reduce the RSV-induced apoptosis of PC-3 cells and also did not further alter the apoptosis status of RWPE cells (Figures 8a and 8b; Supplementary Figure S7). This result indicates that Akt does not play a role in the protection of the RWPE cells against RSV-induced apoptosis.

Discussion

Our current study establishes the anti-cancer oncolytic activity of RSV. In an *in vitro* prostate cancer cellular model and in an *in vivo* xenograft prostate tumor model, we show that the RSV infection rate is markedly enhanced in the cancer cells, but not in the non-cancerous cells. The selective increase of viral burden in the infected cancer cells led to the loss of cell viability, whereas the non-cancerous cells were protected from the virus-induced apoptosis. The *in vitro* results were validated in a human prostate cancer xenograft model in nude mice, which showed significant tumor regression in response to I.T or I.P administration of RSV. We further demonstrated that RSV-mediated oncolysis is due to apoptosis, induced primarily by the mitochondria-mediated activation of the intrinsic pathway involving caspase-3 activation, in association with impaired NF-κB activity.

Clinical trials show promising results with several oncolytic viruses. Oncolytic paramyxoviruses (RSV is a paramyxovirus) such as NDV and measles are currently undergoing successful clinical trials (7–9). Ability of RSV to replicate slowly in normal (non-transformed cells) cells, without causing cell death has been reported (41). Nevertheless, our study is the first demonstration that RSV possesses oncolytic activity. RSV is especially advantageous as an oncolytic virus based on the following rationale: **1)** RSV confers mild respiratory illness in infants and children, while infection is asymptomatic in adults (5, 6). The asymptomatic nature of RSV is borne out by routine intra-nasal infection of live (wild-type) RSV to human subjects enrolled in clinical studies. **2)** RSV does not cause systemic infection due to its respiratory tract-specific entrance into lung epithelial cells via the apical domain of the airway lumen (5, 42) and to date; RSV has not been detected in the serum samples from infected individuals. This is a desirable property for cancer treatment, because systemic delivery of RSV is expected to destroy only tumor cells while keeping the normal cells intact, hence causing limited toxicity to normal tissues. **3)** Since RSV replication occurs in the cytoplasm of the infected cells (5), its transforming potential due to genetic recombination is avoided. **4)** Immune response against RSV is not robust accounting for non-symptomatic re-infection throughout the viral life cycle (5). **5)** The RSV genetic makeup of only ten genes facilitates its manipulation by reverse genetics (43), which would allow us to engineer attenuated RSV-based *efficient and safe* vectors for anti-cancer therapy. **6)** Systemic delivery of RSV should be a viable strategy for targeting tumor cell-specific apoptosis, since our results show that I.P injection of RSV can cause prostate tumor regression in mice (Figure 2c). Even with systemic administration, RSV specifically targeted the tumor mass and conferred its oncolytic activity (Figure 3). Our I.P result suggests that administration of RSV via I.P route results in specific targeting of RSV to the tumor, where high viral multiplicity results in cell death. In contrast, RSV fails to

infect organs such as lungs, liver etc, since the normal cells of these organs may launch an effective anti-viral response to clear virus infection rapidly. Therefore, we failed to detect RSV in these organs; whereas high viral titer was observed in the tumor following I.P injection (Fig. 3b,3c,3d).

Advanced-stage cancer cells including androgen-independent prostate cancer cells (like PC-3) are resistant to apoptosis. Thus, development of therapeutic agents that would induce apoptosis in these cells to cause tumor regression has been a major challenge. Our results reveal that RSV confers its anti-tumor oncolytic activity to PC-3 prostate cancer cells by inducing apoptosis. RSV-mediated apoptosis of PC-3 cells utilized both the mitochondria-mediated intrinsic pathway and the death-receptor-mediated extrinsic pathway, although the former is the major apoptotic trigger in our experimental model (Figure 9).

We show that RSV infection of prostate cancer PC-3 cells result in the suppression of NF-κB activity leading to the up-regulation of pro-apoptotic proteins and down-regulation of anti-apoptotic proteins. Cleavage of pro-caspase-3 also occurs in virus-infected cells. Studies with caspase-specific inhibitors confirmed these observations, since apoptosis was significantly reduced in the presence of caspase-3 and -9 inhibitors. Although the intrinsic pathway constitutes the major route to apoptosis in infected cells, a minor role of the extrinsic pathway in the induction of apoptosis was also observed, especially with regard to caspase-8, which was activated by TNF secreted from infected cells.

Earlier studies failed to notice robust apoptosis of PC-3 cells in response to TNF (44, 45). Our result (Figure 5c) showing approximately 15% contribution of TNF to the apoptotic signaling is similar to previous reports that 15%–20% of PC-3 cells undergo TNF-mediated apoptosis (46). In that context, previous studies (46) have shown that various agents (e.g. cycloheximide) can sensitize TNF to induce apoptosis efficiently (by 50% - 60%) in PC-3 cells. Therefore, we envision similar scenario, whereby RSV infection may enhance the sensitivity of PC-3 cells to undergo TNF-mediated apoptosis. We speculate that RSV infected cells may modulate cellular factors that could enhance the apoptotic potential of TNF. Further studies are required to unravel the mechanism of TNF sensitization in infected cells. Although crosstalk can occur between the extrinsic and intrinsic pathways [via Bid (47)], our results rule out such crosstalk, since the caspase-9 inhibitor reduced apoptosis by 75%, while reduction in the presence of the caspase-8 inhibitor was only 15%. Crosstalk involving two pathways should have caused a significant decline (at least 75%) in apoptosis due to the impaired caspase-9 activation resulting from caspase-8 inhibition. Moreover, so far the ability of caspase-9 to modulate caspase-8 activity has not been demonstrated and our studies demonstrate that such event may not occur since inhibition of caspase-9 did not abolish apoptosis completely (Fig. 5a). If caspase-9 regulated caspase-8 activity, one would expect complete loss of apoptosis activity following caspase-9 inhibition.

Previous studies demonstrated that modulation of both NF-κB and Akt activity by RSV led to apoptosis of lung adenocarcinoma epithelial cells and granulocytes (36, 37). However, our results show that NF-κB activity in RSV-infected prostate cells is important in order to maintain the anti-apoptotic status, since loss of NF-κB activation led to apoptosis. RSV utilizes this mechanism to suppress NF-κB activity and induce apoptosis in PC-3 cells. Lack

of NF-κB inhibition in the RSV-infected normal RWPE cells prevented apoptosis. In contrast to NF-κB, Akt did not play a role in the RSV-mediated apoptosis of prostate cancer cells.

In summary, our study identifies RSV as an oncolytic virus, since the virus can induce apoptosis of cancerous but not non-cancerous prostate epithelial cells in culture, and in prostate tumor xenografts leading to tumor regression. Insights from our findings should lay the foundation for future work aimed at developing RSV-based virotherapy targeted to the clinical management of metastatic prostate cancer.

Supplementary Material

Refer to Web version on PubMed Central for supplementary material.

Acknowledgments

The work was supported by American Lung Association National Biomedical Research Grant (RG-49629-N) (S. Bose), NIH grants AI069062 (S. Bose), CA129246 (S. Bose and B. Chatterjee), T32-DE14318 (S. Bose and A. Sabbah), grant from University of Texas Health Science Centre - San Antonio Cancer Institute (SACI) (S. Bose and B. Chatterjee), AG10486 (B. Chatterjee), AG19660 (B. Chatterjee), VA Merit Review Grant (B. Chatterjee), and Institutional SALSI Grant (B. Chatterjee). BC is a VA Senior Research Career Scientist. FACS analysis at the Core Facility was supported by the San Antonio Cancer Institute grant from NIH- P30 CA54174. We thank Dr. Mark E. Peeples (Columbus Children's Hospital and Ohio State University) and Dr. Peter L. Collins (NIAID, NIH) for providing the GFP expressing RSV.

Abbreviations

RSV	respiratory syncytial virus
TNF	tumor necrosis factor-α
I.P	intra-peritoneal
I.T	intra-tumoral

References

1. Barber GN. VSV-tumor selective replication and protein translation. Oncogene. 2005; 24:7710–7719. [PubMed: 16299531]
2. Parato KA, Senger D, Forsyth PA, Bell JC. Recent progress in the battle between oncolytic viruses and tumours. Nat Rev Cancer. 2005; 5:965–966. [PubMed: 16294217]
3. Bell JC. Oncolytic viruses: what's next? Curr Cancer Drug Targets. 2007; 7:127–131. [PubMed: 17346103]
4. Stanford MM, McFadden G. Myxoma virus and oncolytic virotherapy: a new biologic weapon in the war against cancer. Expert Opin Biol Ther. 2007; 7:1415–1425. [PubMed: 17727330]
5. Collins, PL.; Chanock, RM.; Murphy, BR.; Knipe, DM.; Howley, PM., editors. Fields Virology. Lippincott Williams & Wilkins; Philadelphia: 2001. p. 1443-1486.
6. Cane, P.; Zuckerman, AJ.; Mushahwar, IK. Perspectives in Medical Virology. Elsevier Science Ltd; Amsterdam: 2006. p. 1-340.
7. Fielding AK. Measles as a potential oncolytic virus. Rev Med Virol. 2005; 15:135–142. [PubMed: 15546127]
8. Lorence RM, Katubig BB, Reichard KW, Reyes HM, Phuangsab A, Sassetti MD, Walter RJ, Peeples ME. Complete regression of human fibrosarcoma xenografts after local Newcastle disease virus therapy. Cancer Res. 1994; 54:6017–6021. [PubMed: 7954437]

9. Lorence RM, Roberts MS, O'Neil JD, Groene WS, Miller JA, Mueller SN, Bamat MK. Phase 1 clinical experience using intravenous administration of PV701, an oncolytic Newcastle disease virus. Curr Cancer Drug Targets. 2007; 7:157–167. [PubMed: 17346107]
10. Meng XW, Lee SH, Kaufmann SH. Apoptosis in the treatment of cancer: a promise kept? Curr Opin Cell Biol. 2006; 18:668–676. [PubMed: 17049222]
11. Vermeulen K, Van Bockstaele DR, Berneman ZN. Apoptosis: mechanisms and relevance in cancer. Ann Hematol. 2005; 84:627–639. [PubMed: 16041532]
12. Kidd VJ. Proteolytic activities that mediate apoptosis. Annu Rev Physiol. 1998; 60:533–573. [PubMed: 9558476]
13. Chu ZL, Pio F, Xie Z, Welsh K, Krajewska M, Krajewski S, Godzik A, Reed JC. A novel enhancer of the Apaf1 apoptosome involved in cytochrome c-dependent caspase activation and apoptosis. J Biol Chem. 2001; 276:9239–9245. [PubMed: 11113115]
14. Budihardjo I, Oliver H, Lutter M, Luo X, Wang X. Biochemical pathways of caspase activation during apoptosis. Annu Rev Cell Dev Biol. 1999; 15:269–290. [PubMed: 10611963]
15. Franke TF, Hornik CP, Segev L, Shostak GA, Sugimoto C. PI3K/Akt and apoptosis: size matters. Oncogene. 2003; 22:8983–8998. 2005. [PubMed: 14663477]
16. Barkett M, Gilmore TD. Control of apoptosis by Rel/NF-kappaB transcription factors. Oncogene. 1999; 18:6910–6924. [PubMed: 10602466]
17. Bischoff JR, Kirn DH, Williams A, Heise C, Horn S, Muna M, Ng L, Nye JA, Sampson-Johannes A, Fattaey A, McCormick F. An adenovirus mutant that replicates selectively in p53-deficient human tumor cells. Science. 1996; 274(5286):373–6. [PubMed: 8832876]
18. Harada N, Maniwa Y, Yoshimura M, Nagata M, Hamada H, Yokono K, Okita Y. E1B-deleted adenovirus replicates in p53-deficient lung cancer cells due to the absence of apoptosis. Oncol Rep. 2005; 5:1155–63. [PubMed: 16211279]
19. Chatterjee B. The role of the androgen receptor in the development of prostatic hyperplasia and prostate cancer. Mol Cell Biochem. 2003; 253:89–101. [PubMed: 14619959]
20. Suh J, Rabson AB. NF-kappaB activation in human prostate cancer: important mediator or epiphenomenon? J Cell Biochem. 2004; 91(1):100–17. [PubMed: 14689584]
21. Suh J, Payvandi F, Edelstein LC, Amenta PS, Zong WX, Gélinas C, Rabson AB. Mechanisms of constitutive NF-kappaB activation in human prostate cancer cells. Prostate. 2002; 52(3):183–200. [PubMed: 12111695]
22. Coppe JP, Itahana Y, Moore DH, Bennington JL, Desprez PY. Id-1 and Id-2 proteins as molecular markers for human prostate cancer progression. Clin Cancer Res. 2004; 10:2044–2051. [PubMed: 15041724]
23. Yang M, Jiang P, Sun FX, Hasegawa S, Baranov E, Chishima T, Shimada H, Moossa AR, Hoffman RM. A fluorescent orthotopic bone metastasis model of human prostate cancer. Cancer Res. 1999; 59:781–786. [PubMed: 10029062]
24. Bose S, Kar N, Maitra R, DiDonato JA, Banerjee AK. Temporal activation of NF-κB regulates an interferon-independent innate antiviral response against cytoplasmic RNA viruses. Proc Natl Acad Sci USA. 2003; 100:10890–10895. [PubMed: 12960395]
25. Bose S, Basu M, Banerjee AK. Role of nucleolin in human parainfluenza virus type 3 infection of human lung epithelial cells. J Virol. 2004; 78:8146–8158. [PubMed: 15254186]
26. Kota S, Sabbah A, Chang TH, Harnack R, Xiang Y, Meng Y, Bose S. Role of Human β-Defensin-2 during Tumor Necrosis Factor-α/NF-κB-mediated Innate Antiviral Response against Human Respiratory Syncytial Virus. J Biol Chem. 2008; 283:22417–22429. [PubMed: 18567888]
27. Pauwels R, Balzarini J, Baba M, et al. Rapid and automated tetrazolium-based colorimetric assay for the detection of anti-HIV compounds. J Virol Methods. 1988; 20:309–21. [PubMed: 2460479]
28. Murugananandham M, Alfieri AA, Matei C, Chen Y, Sukenick G, Schemainda I, Hasmann M, Saltz LB, Koutcher JA. Metabolic signatures associated with a NAD synthesis inhibitor-induced tumor apoptosis identified by 1H-decoupled-31P magnetic resonance spectroscopy. Clin Cancer Res. 2005; 11:3503–3513. [PubMed: 15867253]
29. Bose S, Malur A, Banerjee AK. Polarity of human parainfluenza virus type 3 infection in polarized human lung epithelial A549 cells: role of microfilament and microtubule. J Virol. 2001; 75:1984–1989. [PubMed: 11160698]

30. Jounaidi Y, Waxman DJ. Use of replication-conditional adenovirus as a helper system to enhance delivery of P450 prodrug-activation genes for cancer therapy. Cancer Res. 2004; 64:292–303. [PubMed: 14729637]
31. Hallak LK, Collins PL, Knudson W, Peeples ME. Iduronic acid-containing glycosaminoglycans on target cells are required for efficient respiratory syncytial virus infection. Virology. 2000; 271:264–275. [PubMed: 10860881]
32. Szegezdi E, Fitzgerald U, Sanamali A. Caspase-12 and ER-stress-mediated apoptosis: the story so far. Ann N Y Acad Sci. 2003; 1010:186–194. [PubMed: 15033718]
33. Bitko V, Barik S. An endoplasmic reticulum-specific stress-activated caspase (caspase-12) is implicated in the apoptosis of A549 epithelial cells by respiratory syncytial virus. J Cell Biochem. 2001; 80:441–454. [PubMed: 11135374]
34. Kim KB, Choi YH, Kim IK, Chung CW, Kim BJ, Park YM, Jung YK. Potentiation of Fas-and TRAIL-mediated apoptosis by IFN-gamma in A549 lung epithelial cells: enhancement of caspase-8 expression through IFN-response element. Cytokine. 2002; 20:283–288. [PubMed: 12633570]
35. Jiang Z, Kunimoto M, Patel JA. Autocrine regulation and experimental modulation of interleukin-6 expression by human pulmonary epithelial cells infected with respiratory syncytial virus. J Virol. 1998; 72:2496–2499. [PubMed: 9499112]
36. Thomas KW, Monick MM, Staber JM, Yarovinsky T, Carter AB, Hunninghake GW. Respiratory syncytial virus inhibits apoptosis and induces NF-kappa B activity through a phosphatidylinositol 3-kinase-dependent pathway. J Biol Chem. 2002; 277:492–501. [PubMed: 11687577]
37. Lindemans CA, Coffer PJ, Schellens IM, de Graaff PM, Kimpen JL, Koenderman L. Respiratory syncytial virus inhibits granulocyte apoptosis through a phosphatidylinositol 3-kinase and NF-kappaB-dependent mechanism. J Immunol. 2006; 176:5529–5537. [PubMed: 16622022]
38. Mori A, Lehmann S, O'Kelly J, Kumagai T, Desmond JC, Pervan M, McBride WH, Koeffler HP. Capsaicin, a component of red peppers, inhibits the growth of androgen-independent, p53 mutant prostate cancer cells. Cancer Res. 2006; 66:3222–3229. [PubMed: 16540674]
39. Orlandi A, Francesconi A, Marcellini M, Di Lascio A, Spagnoli LG. Propionyl-L-carnitine reduces proliferation and potentiates Bax-related apoptosis of aortic intimal smooth muscle cells by modulating nuclear factor-kappaB activity. J Biol Chem. 2007; 282:4932–4942. [PubMed: 17178728]
40. Naderi A, Teschendorff AE, Beigel J, Cariati M, Ellis IO, Brenton JD, Caldas C. BEX2 is overexpressed in a subset of primary breast cancers and mediates nerve growth factor/nuclear factor-kappaB inhibition of apoptosis in breast cancer cell lines. Cancer Res. 2007; 67:6725–6736. [PubMed: 17638883]
41. Zhang L, Peeples ME, Boucher RC, Collins PL, Pickles RJ. Respiratory syncytial virus infection of human airway epithelial cells is polarized, specific to ciliated cells, and without obvious cytopathology. J Virol. 2002; 76:5654–5666. [PubMed: 11991994]
42. Roberts SR, Compans RW, Wertz GW. Respiratory syncytial virus matures at the apical surfaces of polarized epithelial cells. J Virol. 1995; 69:2667–2673. [PubMed: 7884920]
43. Murphy BR, Collins PL. Live-attenuated virus vaccines for respiratory syncytial and parainfluenza viruses: applications of reverse genetics. J Clin Invest. 2002; 110:21–27. [PubMed: 12093883]
44. Yu R, Mandlekar S, Ruben S, Ni J, Kong AN. Tumor necrosis factor-related apoptosis-inducing ligand-mediated apoptosis in androgen-independent prostate cancer cells. Cancer Res. 2000; 60:2384–2389. [PubMed: 10811114]
45. Subbarayan V, Sabichi AL, Llansa N, Lippman SM, Menter DG. Differential expression of cyclooxygenase-2 and its regulation by tumor necrosis factor-alpha in normal and malignant prostate cells. Cancer Res. 2001; 61:2720–2726. [PubMed: 11289153]
46. Rong, Yu; Sandhya, Mandlekar; Steve, Ruben; Jian, Ni A-N.; Tony, Kong. Tumor Necrosis Factor related Apoptosis-inducing Ligand-mediated Apoptosis in Androgen-independent Prostate Cancer Cells. Cancer Research. 2000; 60:2384–2389. [PubMed: 10811114]
47. Roy S, Nicholson DW. Cross-talk in cell death signaling. J Exp Med. 2000; 192:F21–F25. [PubMed: 11034612]

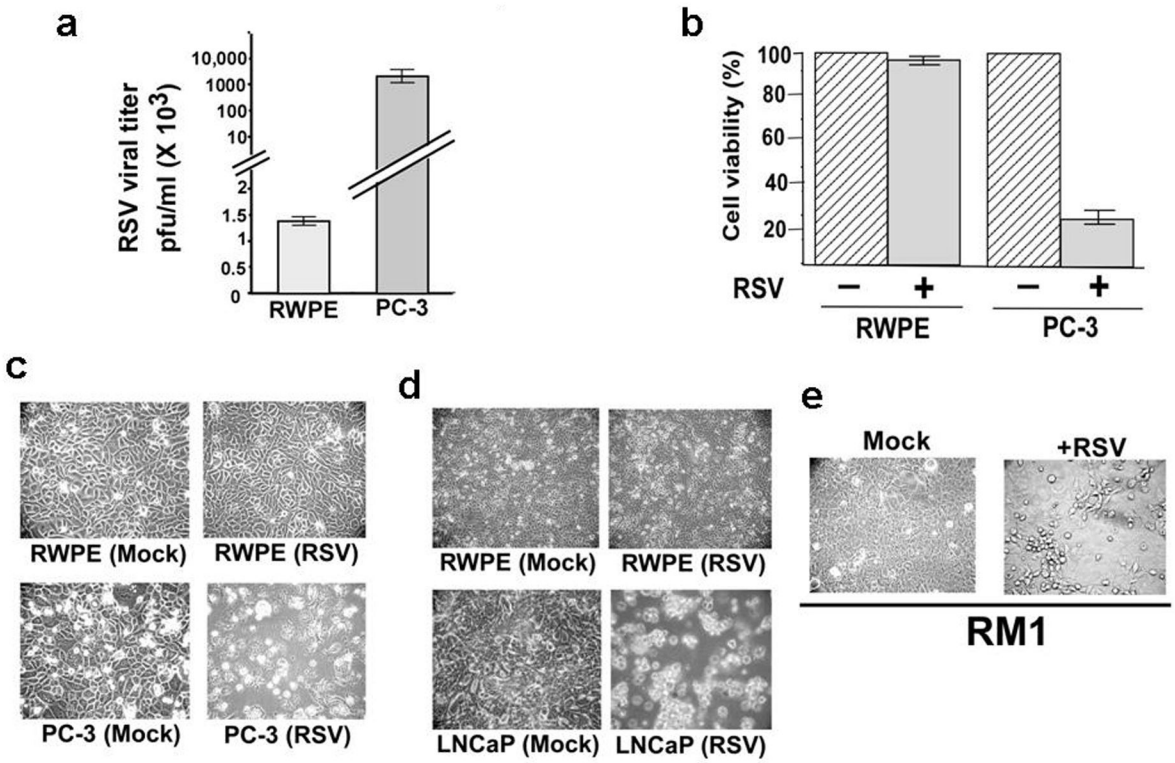

Figure 1.

RSV infectivity in RWPE-1 (RWPE) and PC-3 cells. **(a)** RSV infection measured by plaque assay at 36 h post-infection. **(b)** MTT cell viability assay of cells infected with RSV for 36h. MTT assay values are mean ± standard deviation of 6 wells and triplicate experiments. Uninfected (-) cells indicate 100% cell viability. **(c)** Morphology of mock-infected or RSV-infected RWPE and PC-3 cells at 24h post-infection. **(d)** Morphology of mock-infected or RSV-infected RWPE and LNCaP cells at 10h post-infection. **(e)** Morphology of mock-infected or RSV-infected mouse prostate cancer RM1 cells at 18h post-infection. Plaque assay values expressed as pfu/ml represent mean ± standard deviation for three independent determinations. Standard deviations are shown by the error bars.

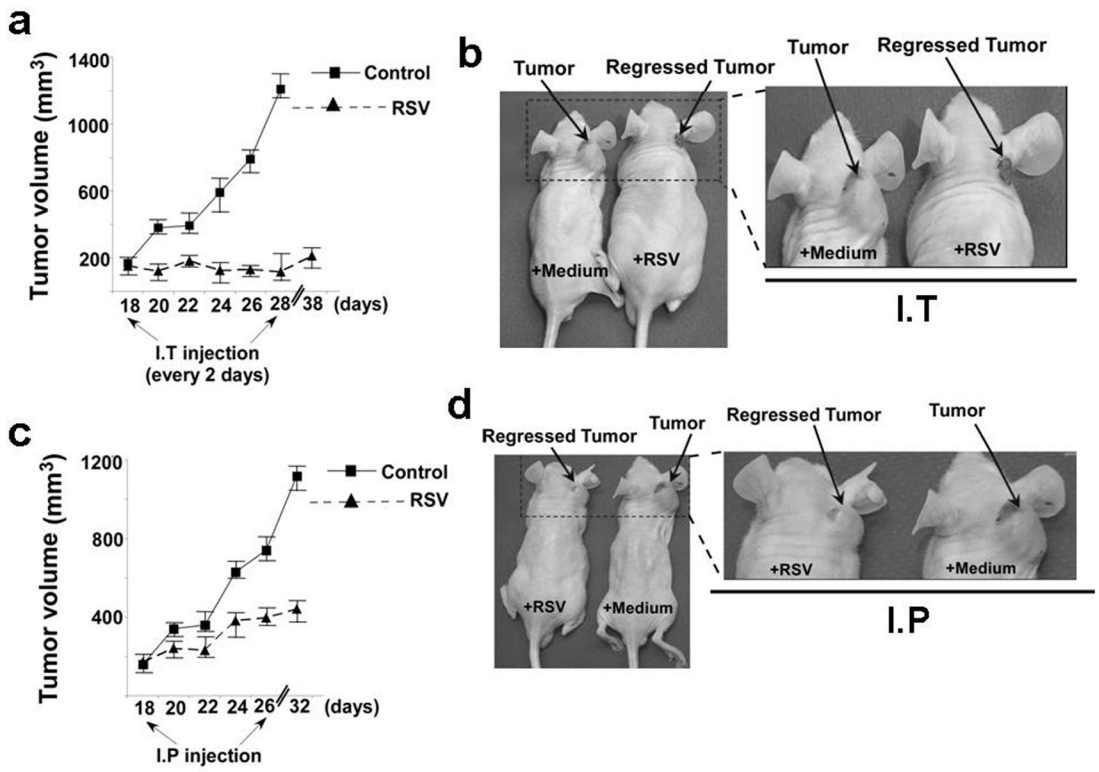

Figure 2.

Prostate tumor growth in nude mice following RSV administration. **(a)** Effect of intra-tumorally (I.T) administered RSV or control medium on tumor growth in mice harboring the tumor xenograft below the ear. **(b)** Tumor regression at the ear site after intra-tumoral injection of RSV. The boxed area at the left panel is enlarged in the right panel. **(c)** Effect of intra-peritoneal (I.P) administration of RSV or control medium on tumor growth in mice harboring the tumor xenograft below the ear. **(d)** Tumor regression at the ear site after I.P injection of RSV. The boxed area at the left panel is enlarged in the right panel. Tumors were allowed to develop first. At day 18 RSV injections was initiated. Injection was given every 2 days for the period shown in the plot. For data shown in Figures 2a and 2c, each treatment group consisted of five animals (n=5) and the data represent the mean and standard deviation of each group. The complete experiment has been repeated twice with similar results.

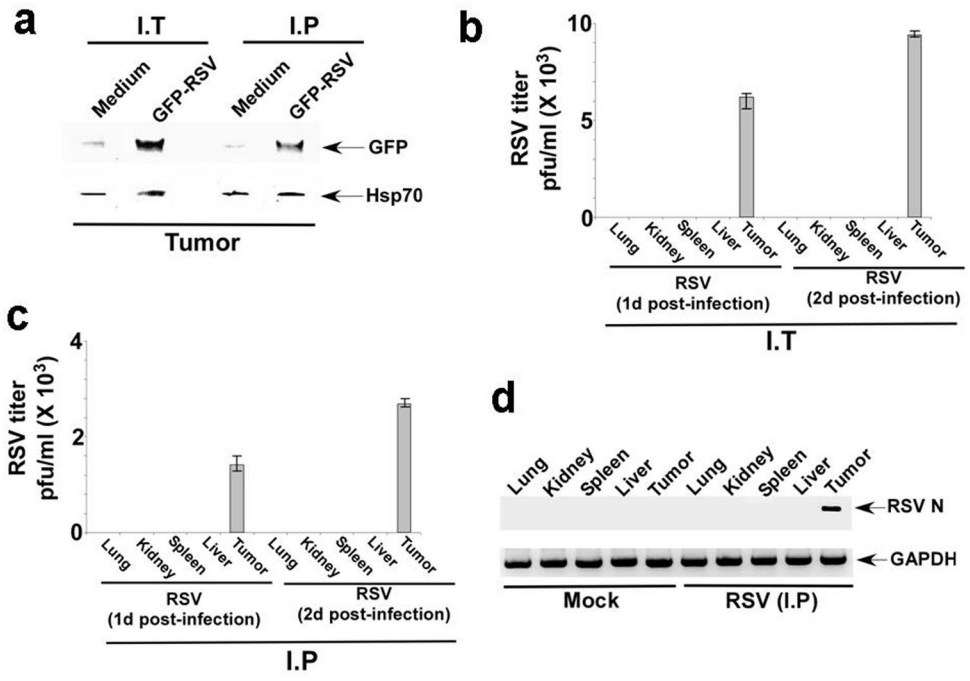

Figure 3.

Localization of RSV in prostate tumors. **(a)** Mice harboring the tumor xenograft below the ear were injected with medium (control) or infected (via I.T or I.P) with GFP expressing RSV (GFP-RSV). At 16h post-infection, the tumors from control (medium) and infected (GFP-RSV) mice were surgically excised following euthanasia. The tumor homogenate (100 μg protein) was then subjected to Western blot analysis with anti-GFP and anti-Hsp70 (loading control) antibodies. Mice harboring the tumor xenograft below the ears were administered RSV via I.T **(b)** or I.P **(c)** and at 1d or 2d post-infection, tumors and various organs were surgically removed from the animals. The homogenate prepared from the organs and tumors were subjected to plaque assay analysis to measure viral titer. Plaque assay values expressed as pfu/ml represent mean ± standard deviation for three independent determinations and the standard deviations are shown by the error bars. **(d)** Mice harboring the tumor xenograft below the ears were administered RSV via I.P and at 1d post-infection; tumors and various organs were surgically removed from the animals. The RNA isolated from various organs and tumors were subjected to RT-PCR analysis for RSV nucleocapsid (N) protein expression.

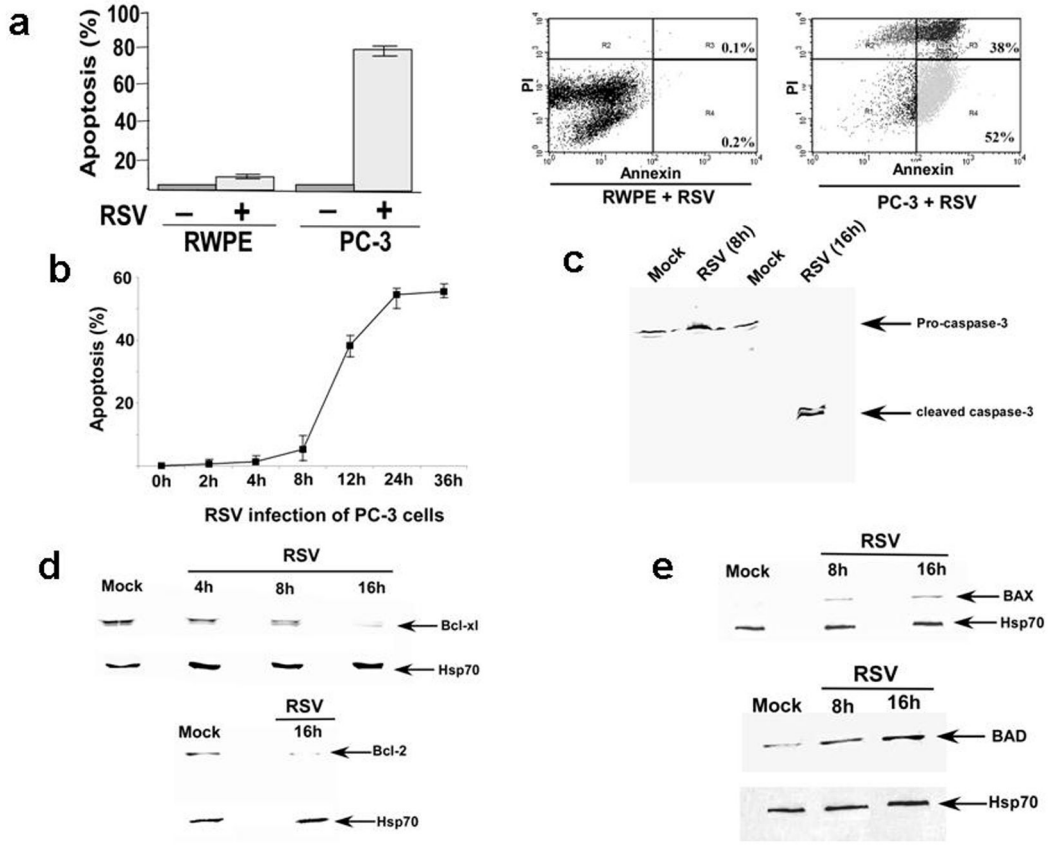

Figure 4.

Role of mitochondria-mediated (intrinsic) pathway in apoptosis of RSV infected PC-3 cells. **(a)** left panel- TUNEL assay for apoptosis analysis of RSV infected RWPE-1 (RWPE) and PC-3 cells at 36h post-infection. % apoptotic cells were calculated based on the total number of cells present during each experimental set. Apoptotic values represent mean ± SD for three determinations. Right panel – Annexin V/propidium iodide (PI) assay of RWPE and PC-3 cells infected with RSV for 24h. The cells present in the upper-right and lower-right corner of the quadrant represents late (PI staining) and early (annexin staining) apoptotic events, respectively. **(b)** Kinetics of apoptotic induction was examined by infecting PC-3 cells with RSV for 0h-36h, followed by analyzing apoptosis by annexin V/PI assay. % Apoptosis represents the % of cells that are undergoing early apoptosis (i.e. positive for annexin V staining). The values represent mean ± SD for three determinations. **(c)** PC-3 cell lysates obtained from mock and RSV infected (8h and 16h post-infection) cells were subjected to Western blot analysis with caspase-3 antibody that detects both full-length and cleaved caspase-3 protein. **(d)** PC-3 cell lysates obtained from mock and RSV infected (8h and 16h post-infection) cells were subjected to Western blot analysis with Bcl-2 (bottom) and Bcl-xL (top) antibodies. **(e)** PC-3 cell lysates obtained from mock and RSV infected (8h and 16h post-infection) cells were subjected to Western blot analysis with Bad (bottom), Bax (top). Hsp70 antibodies were used for loading controls. Mock; un-infected cells.

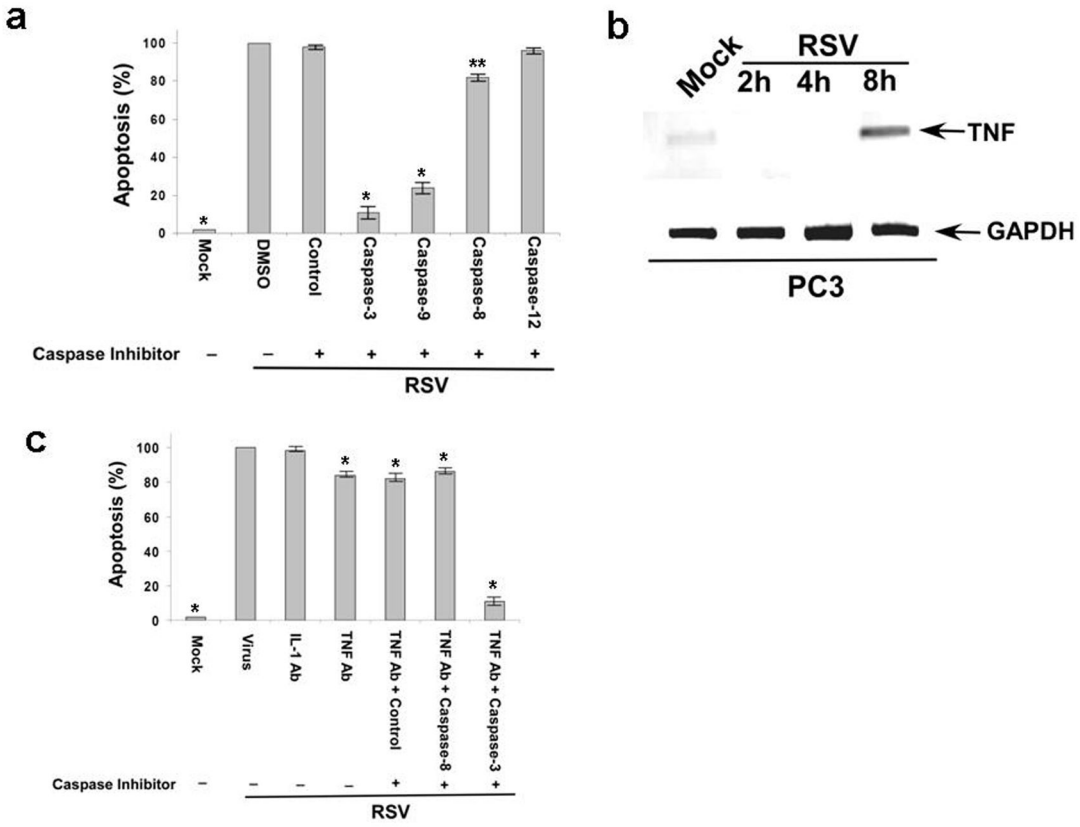

Figure 5.

Role of intrinsic, extrinsic (death-receptor dependent) and ER-stress pathway in RSV mediated apoptosis in PC-3 cells. **(a)** PC-3 cells infected in the presence of DMSO, control caspase inhibitor (Control) and caspase-3, -9, -8 and -12 inhibitors were subjected to apoptosis assay at 36h post-infection. **(b)** RT-PCR analysis of human TNF expression in PC-3 cells infected with RSV for 2h–8h. **(c)** PC-3 cells infected in the absence (virus only) or presence of neutralizing antibodies [either interleukin-1β (IL-1 Ab) or tumor necrosis factor-α (TNF Ab) neutralizing antibodies], control or caspase (caspase-3 or -8) inhibitors were subjected to apoptosis assay at 36h post-infection. In Figures 5a and 5c, % apoptotic cells were calculated based on the total number of cells present during each experimental set. Apoptotic values represent mean ± SD for three determinations. Dunnett's two-sided SCI Test was employed to reveal the statistical difference between the DMSO mean and the mean of other treatment groups (**: p=0.05, *: p=0.01) (5a) and between virus mean and the mean of other treatment groups (*: p=0.01) (5c). Mock; un-infected cells.

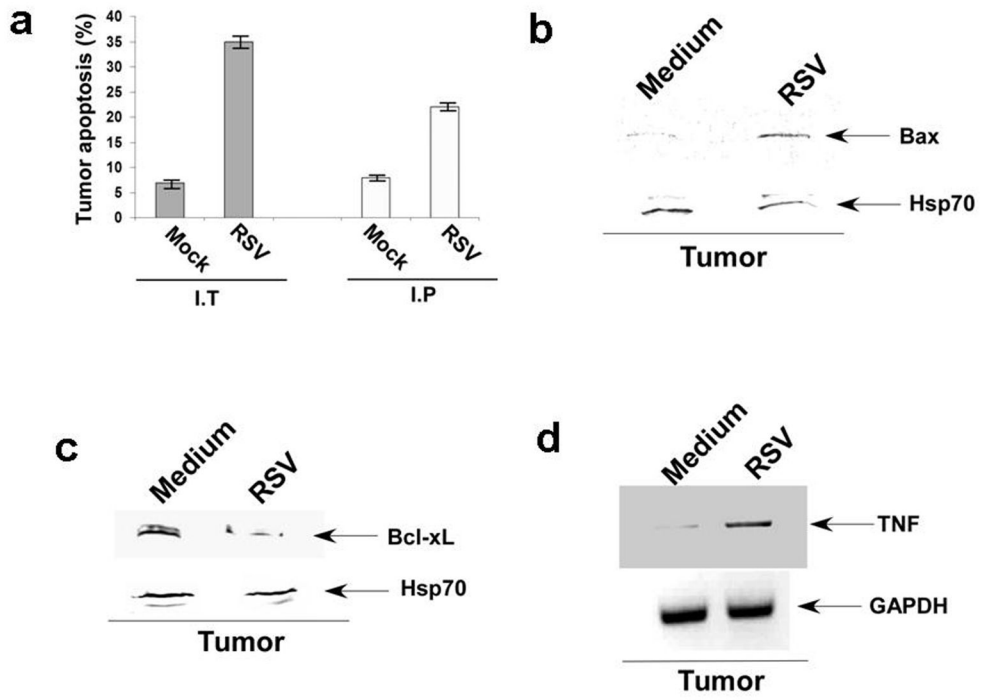

Figure 6.

RSV mediated *in vivo* apoptosis of prostate tumors. **(a)** Cell suspension prepared from tumors surgically excised from mock infected or RSV infected (via I.T or I.P) mice were stained with annexin V and propidium iodide to measure apoptosis. The % apoptotic cells indicate the number of cells in each experimental set undergoing apoptosis. The values represent mean ± SD for three determinations. **(b)** The tumor homogenate obtained from mice infected with RSV (via I.T) was subjected to Western blot analysis with Bax and Hsp70 antibodies. **(c)** The tumor homogenate obtained from mice infected with RSV (via I.T) was subjected to Western blot analysis with Bcl-xL and Hsp70 antibodies. **(d)** RT-PCR analysis of murine TNF expression in tumors obtained from RSV infected (via I.T) mice. Medium; Tumor derived from control mice injected with medium alone.

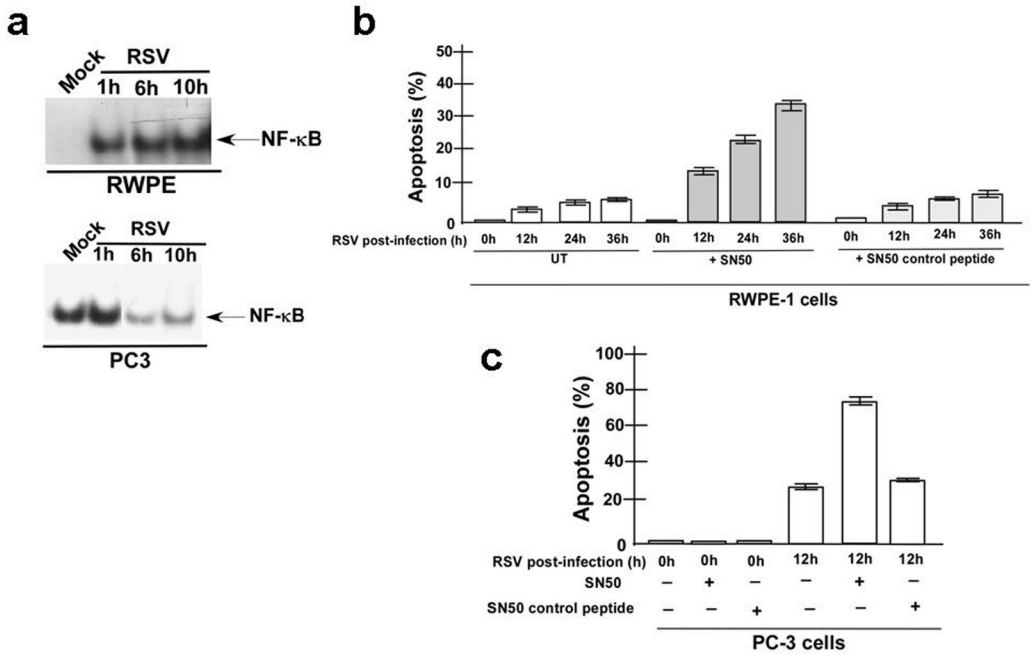

Figure 7.

Role of NF-κB in apoptosis of RSV infected prostate cells. **(a)** NF-κB specific EMSA of nuclear extracts prepared from mock infected and RSV infected RWPE-1 (RWPE) and PC-3 cells. **(b)** RWPE cells infected with RSV in the absence (untreated, UT) or presence of either SN50 peptide or control SN50M peptide were subjected to apoptosis assay. **(c)** PC-3 cells infected with RSV in the absence (−) or presence (+) of either SN50 peptide or control SN50M peptide for 0h and 12h were subjected to apoptosis assay.

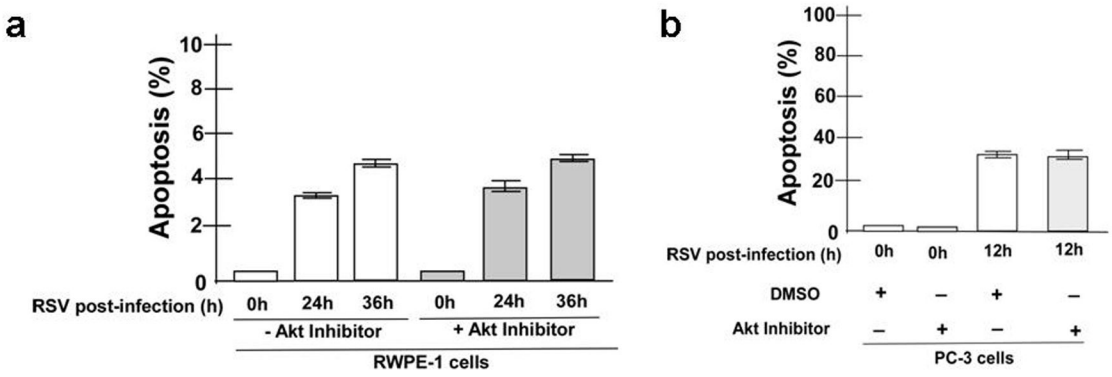

Figure 8.

Role of Akt in anti-apoptotic function of RSV infected RWPE and PC-3 cells. **(a)** RWPE cells infected in the presence of DMSO (control) (−Akt inhibitor) or Akt inhibitor (+Akt inhibitor) (20 μM) for 0h, 24h and 36h were subjected to apoptosis assay. % apoptotic cells were calculated based on the total number of cells present during each experimental set. Apoptotic values represent mean ± SD for three determinations. **(b)** PC-3 cells infected in the presence of DMSO or Akt inhibitor for 0h, 24h and 36h were subjected to apoptosis assay as described above for RWPE cells. % apoptotic cells were calculated based on the total number of cells present during each experimental set. Apoptotic values represent mean ± SD for three determinations.

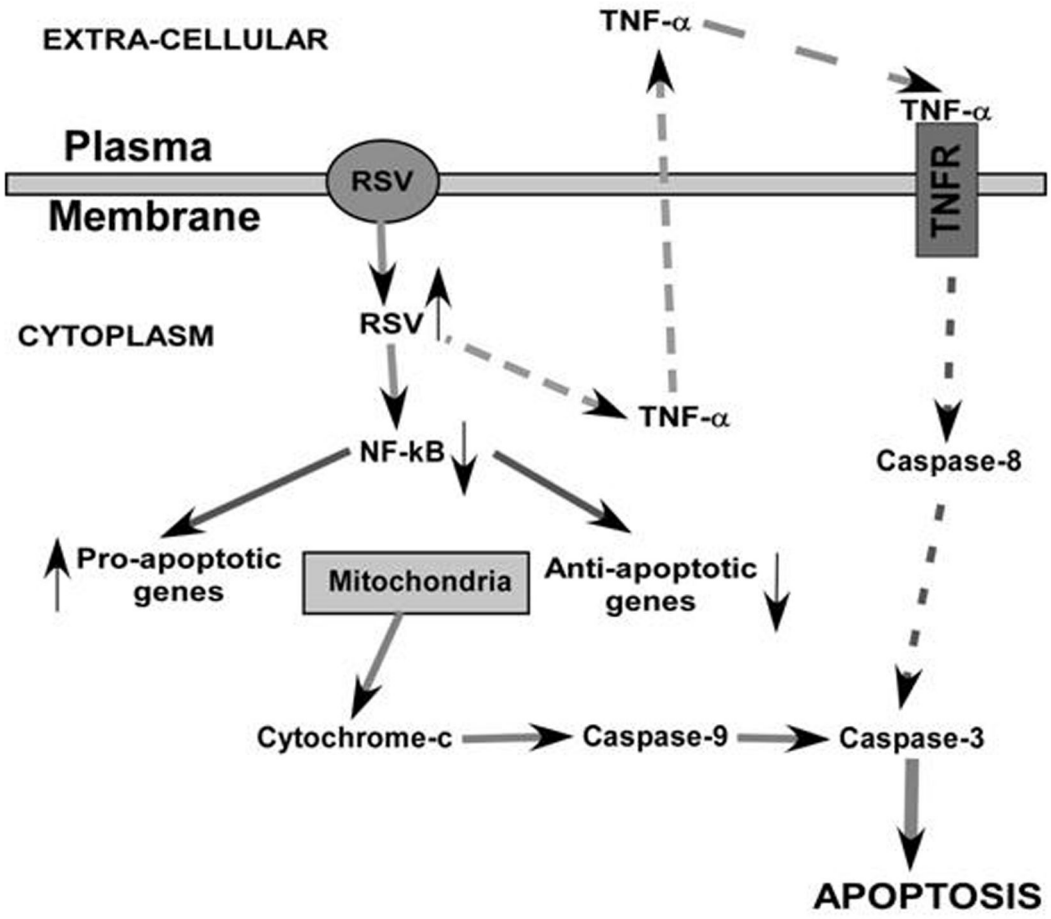

Figure 9.

A model depicting mechanism of apoptosis in RSV infected prostate cells. Model for the mechanism of apoptosis in RSV infected PC-3 prostate cancer cells – apoptosis occur in PC-3 cells due to high (↑) level of RSV infectivity and inhibition (↓) of NF-κB activity following RSV infection. NF-κB inhibition results in down-regulation (↓) of anti-apoptotic molecules and activation (↑) of pro-apoptotic proteins. The major mechanism (shown with solid arrows) comprises of activation of mitochondria-dependent intrinsic pathway: the pathway that is activated following induction (↑) of pro-apoptotic proteins [and suppression (↓) of anti-apoptotic proteins] leading to change in mitochondrial membrane potential and release of cytochrome-c which can activate caspase-9. Active caspase-9 then activates the "executioner" caspase, caspase-3 to induce apoptosis. The minor mechanism (shown with broken arrows) involves induction of death-domain-mediated extrinsic pathway; which is accomplished via the paracrine/autocrine action of TNF-α (upon binding to the TNF-α receptor/TNFR) produced from infected cells. Binding of TNF-α to its receptor (TNFR) results in activation of caspase-8; which in turn activates caspase-3 leading to apoptosis.